Publication V

V

Foda E, Sirén K. Design strategy for maximizing the energy-efficiency of a localized floor-heating system using a thermal manikin with human thermoregulatory control. Energy and Buildings 51: 111-121. 2012.

Energy and Buildings 51 (2012) 111–121

Contents lists available at SciVerse ScienceDirect

Energy and Buildings

journal homepage: www.elsevier.com/locate/enbuild

Design strategy for maximizing the energy-efficiency of a localized floor-heating system using a thermal manikin with human thermoregulatory control

Ehab Foda*, Kai Sirén

Department of Energy Technology, Aalto University, PO Box 14100, Espoo, Finland

ARTICLE INFO

Article history:
Received 15 February 2012
Received in revised form 19 March 2012
Accepted 19 April 2012

Keywords:
Energy saving
Local thermal comfort
Floor-heating
Thermal manikin
TAC systems
Shopping mall

ABSTRACT

Localized HVAC systems with the task-ambient conditioning concept represent a promising option towards energy-saving in buildings. The design of such systems needs to involve evaluation of the local thermal comfort that corresponds to different body segments. In this work, an experimental technique using a thermal manikin was developed to determine the optimum configuration(s) among different variants of localized floor-heating systems for a single seated person. The experimented variants had different geometries or surface areas. Their surface temperatures were experimentally found subject to thermal comfort criteria and under a lowered ambient temperature. In the experiments, the thermal manikin was regulated in a dynamic mode using a model of human thermoregulation and was employed to evaluate the fulfillment of the thermal comfort criteria. The experimental setup was constructed to simulate a task area in a large hall space that may be feasible for shopping mall's application. The energy consumption of the floor-heating systems was measured to evaluate the energy performance of the different system variants. The results showed that in large hall space under lowered ambient temperature around 18 °C, a heated floor with certain geometries and a surface area of nearly 1 m^2 could fulfill the comfort criteria and represented the optimum configuration.

1. Introduction

Task-ambient conditioning (TAC) systems are known for their potential to reduce total energy use by focusing that on local spaces with task-doers while applying moderate conditioning at the ambient. Conventional TAC systems from 1990s were mainly all air systems, for open-plan office spaces. These systems use under floor plenums and floor-based air diffusers; or air-outlets that is integrated with the room furniture. The conditioned air from these systems is thrown towards the occupants with individual control enabled for thermal comfort preferences. The evaluation of the local thermal comfort can further assist the design of these localized systems towards energy-saving. This can be realized by focusing the energy use on occupant's body and even on certain body segments based on local comfort criteria. Azer and Nevins [1] showed that the thermal comfort in hot environment could be improved, using an overhead cool air jet, respectively from hot to warm and from very uncomfortable to uncomfortable. Bauman et al. [2] used a thermal manikin to evaluate the local thermal comfort and optimize the performance of a floor-based TAC system. Finally they introduced general recommendations to improve the performance of that system type. Amai et al. [3] used human subjects to evaluate the local thermal comfort; and hence, the performance of 4 different TAC systems. The subjects' preferable directions of the supply air were different with each system; however, the individual control of those TAC systems contributed well to make the preferred environment. Arens et al. [4,5], in a two-part paper, stated that hands and feet feel cooler than other body segments in cool environments while the head (excluding the breathing zone) is more sensitive to warm conditions than the rest of the body segments. This was based on large-scale human subjects' tests performed at the University of California, Berkeley (UCB). The UCB research team made use of these results to develop an un-conventional TAC system integrated with a workstation and focused on the body's thermally sensitive segments [6]. The TAC system consisted of: palm warmer and hand ventilation device integrated with the computer's keyboard; under-desk feet warmer; and a head-ventilation device. The thermal comfort was evaluated for that TAC system at ambient temperatures from 18 to 30 °C using 18 human subjects. The results showed that with such a low-power system the thermal comfort level of subjects was improved by the system especially when enabling the subjects to control the heating level. Watanabe et al. [7] introduced another un-conventional TAC system uses a chair equipped with fans that is individually controlled. Human subjects were used to evaluate the thermal comfort performance of that system. The ambient temperature was set at 26 °C, 28 °C, 30 °C

* Corresponding author. Tel.: +358 947023598; fax: +358 947023611.
E-mail address: ehab.foda@aalto.fi (E. Foda).

0378-7788/$ – see front matter © 2012 Elsevier B.V. All rights reserved.
http://dx.doi.org/10.1016/j.enbuild.2012.04.019

and 32 °C. The subjects reported an acceptable thermal comfort level up to 30 °C ambient temperature.

Radiant heating and cooling systems accompanied with a general ventilation system may also form more variants of TAC systems. While the use of a radiant-heating panel is an optional heating source in some of the introduced TAC systems, Sørlie et al. [8] used that alone mounted under the occupant's desk. They reported acceptable overall thermal comfort with 60 W heater output under ambient temperature around 17–18 °C. In that study, a thermal manikin was used to verify only the overall thermal comfort based on whole-body heat loss.

Generally, most of the introduced TAC systems were all air systems, with a high initial cost and focused on the office building's application. The concept of TAC systems can further be utilized in other applications such as the shopping mall's application. A shopping mall represents an integrated complex of shops and large spaces under the same ceiling hosting different nature of business and various activities. Shopping malls, especially those housing restaurants and food retailers, are buildings with high intensity of energy use. Narrowing our scope to the Scandinavian region with their high heating demand, the average energy use of a typical Scandinavian mall is around 300 kWh/m^2 a. This was estimated based on gathered data from 41 shopping malls in Norway and Sweden by Stensson et al. [9]. The building services including heating, cooling and ventilation energies represent more than 30% of the total energy consumption. The main energy use in these malls is consumed by the tenants especially for shops' lighting. While the tenant's energy demand is usually according to standard setup by international chains and brands, there is a significant potential for improvements in the energy use of the building services. The design of HVAC systems for shopping malls needs to closely consider the different activities and clothing levels of the occupants; and hence, minimizing the used energy by these systems. In the heating-mode season, the occupants usually keep their heavy clothing while moving in corridors and between shops. Therefore, a lowered set-point of the ambient temperature may be acceptable with the general ventilation system of the mall. In accompaniment, localized heating systems need to be employed as required in certain locations such as resting spots including cafés and restaurants. This scheme should promote the thermal comfort of individuals and contribute in saving energy.

In this study, an experimental setup was constructed to simulate a task area in a large hall space that may be feasible for the shopping mall's application. Variants of a localized floor-heating system were used at the task area under lowered ambient conditions. The energy consumption of these variants was measured along with online evaluation of the local and overall thermal comfort using a thermal manikin to evaluate their performance.

2. Methods

2.1. Optimization-based design strategy

Optimization-based design is a used technique to assist the engineering design process. This is by setting clearly the design problem; addressing the objectives and constraints; and providing optimum solutions. The optimum solution may be found by solving the optimization problem in many different ways. In this study, an experimental technique was used to find the optimum configuration(s) among a set of variants of a localized floor-heating system, focused on the geometry surface area and temperature. The optimum surface temperature of each system variant is experimentally found subject to a thermal comfort criteria and a constraint for the allowed maximum temperature. The evaluation of the thermal comfort was carried out using a thermal manikin with human thermoregulatory control. The energy consumption was measured at each case to find the minimum consumption among the experimented variants.

The design problem may be formulated on the shape of an optimization problem to minimize the system power and hence, maximize the energy efficiency of the system:

$$\begin{array}{ll} \text{Min} & P(x, A, T_s, T_{amb}) \\ \text{Subject to} & T_s \le 40 \\ & -1.5 \le \text{LTC} \le 1.5 \\ & I_{CL} = 0.6 \\ & \text{OTC} = -1.5 \end{array} \quad (1)$$

where P is the system power at steady-state operation (W), x is the floor heater geometry, A is the floor heater surface area (m^2), T_s is the floor surface temperature (°C), T_{amb} is the ambient temperature (°C), I_{CL} is the clothing intrinsic thermal resistance (clo = 0.155 m^2 °C/W), LTC is the local thermal comfort index, and OTC is the overall thermal comfort index.

The inequality constraint for the floor surface temperature sets a maximum surface temperature of 40 °C. The selected value of the maximum surface temperature was chosen according to the system's maximum power under 17–18 °C ambient temperature. The value does not follow the given limit of floor's temperature in ISO7730 [10] which may not be applicable for a localized system in such large spaces; and it is going to be evaluated in this study using the local comfort concept. The inequality and equality constraints for the local and overall comfort criteria respectively, are adopted from the comfort zones introduced by Nilsson [11,12]. The equality is used only with the overall thermal comfort and not on segmental basis to ease the comparison between the different variants. Furthermore, the lower limit of the comfort zone (i.e. −1.5) was used in the equality taking into account the light clothing ensemble (0.6 clo) used in these experiments.

2.2. Floor heater variants

In this study, heated floor tiles (60 × 60 cm) were used to form the different floor-heater variants. These variants had different geometries or surface areas as shown in Fig. 1. The black node shown on the figure represents the manikin position on the floor and the dotted rectangles gather the different geometries of variants that have the same surface area. The figure also shows the manikin direction on the floor and a cutaway diagram of the floor tile construction. The tiles were heated using a floor heater cable (Deviflex DTIP-18, Danfoss) that was wound over a 10 cm thick polyurethane grooved-board. This was covered with a 2 mm thick aluminum sheet and parquet finish-floor (as a realistic finish-floor). All layers were tightened using screws from all sides on a 3 cm thick wooden frame. The use of electrical heating, in this study, was to simplify the experimental setup and measurements of energy use; however, the heating of the floor tiles could preferably be based on a hydronic system. In addition, it should be noted that minimizing the energy use by optimizing the construction of the floor tiles was not in the scope of this work; rather, it was thought to be an industrial job. The main focus was to illustrate the methodology and to possibly obtain the optimum geometry, surface area and the needed surface temperature under the given experimental conditions in the hall space.

2.3. Thermal manikin

The thermal manikin 'Therminator' is a European male size 50 that can stand, sit, move his arms and breathe. It consists of 24 body segments that can be individually heated and set at a target value. The manikin thermoregulatory control is based on the multisegmental Pierce (*MSP*) model of human thermoregulation [13].

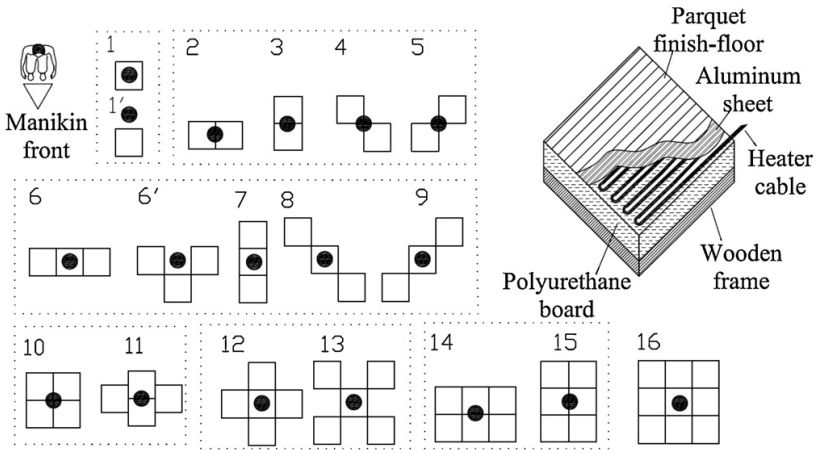

Fig. 1. Different variants of the floor heater and a cutaway diagram of the floor tile.

This thermoregulatory control mode was implemented onto the manikin's system, in earlier work [14], using LabVIEW platform and was validated for the estimation of the local (segmental) thermal comfort using the equivalent temperature (t_{eq}) approach [15].

In this study, the manikin's program on LabVIEW was modified to use the *MSP* control in a dynamic mode for real-time measurements and present correspondent estimation of the local thermal comfort as well as the room physical parameters on the system's front panel. Fig. 2 shows a flowchart of the manikin's control system. The *MSP* model was used to calculate the steady-state skin temperatures during the manikin's warming-up period to set the initial values for the dynamic mode with the real-time measurements. The segmental set-points were updated at 1 min time step based on the averaged environmental measurements over that interval.

2.4. The equivalent temperature (t_{eq}) approach

The t_{eq} approach was first introduced by Wyon et al. [15] for assessing the vehicle climate using a thermal manikin. Wyon and Sandberg [16] used the same approach in evaluating local thermal discomforts due to vertical temperature gradients in buildings and it was then used in a several studies evaluating buildings. The t_{eq} approach is a feasible method for laboratory and real-life measurements evaluating thermal comfort of sedentary people. The segmental and overall t_{eq} are calculated, from thermal manikin experiments, using the following equation [11]:

$$t_{eq} = t_{sk} - \frac{Q_s}{h_{cal}} \quad (^\circ\mathrm{C}) \tag{2}$$

where t_{sk} is the manikin skin temperature (°C), Q_s is the manikin sensible (dry) heat loss (W/m^2), h_{cal} is the heat transfer coefficient from calibrations under uniform and calm conditions (W/m^2 K).

Wyon et al. [15] presented the t_{eq} on a diagram that shows the so-called ideal profile (neutral) and acceptable ranges (mean vote = ±0.8 corresponds to 20% dissatisfied) for the different body segments. A new diagram, called comfort zone diagram, with a wider acceptable ranges (mean vote = ±1.5) was later obtained by Nilsson [11,12] from subjective assessments in more than 30 sets of climatic conditions. The t_{eq} at these conditions was estimated using two thermal manikins (with the constant surface temperature "*CST*" control mode at 34 °C) and correlated with the mean votes from the subjective tests. The following correlation was then introduced for each body segment and for whole body to construct the comfort zones [11,12]:

$$t_{eq} = t_{sk} - R_T \times (a + b \times MTV) \quad (^\circ\mathrm{C}) \tag{3}$$

where R_T is the clothing total thermal resistance (m^2 K/W), a and b are the linear regression coefficients given in Nilsson's study [12], t_{sk} is the manikin's skin temperature (i.e. 34 °C in Nilsson's correlation), *MTV* is the mean thermal comfort vote.

Table 1 shows the suggested mean vote ranges of comfort zones by Nilsson and correspondent sensations that are based on the 7-point Bedford scale [17]. In this study, this was used to present the results from the manikin measurements and indicate the local and overall thermal sensations. The thermal comfort indices LTC and OTC were calculated using Eq. (3) as the *MTV*'s by substituting the measured segmental and overall t_{eq} respectively along with other parameters. Accordingly, Eq. (3) may be rewritten as:

$$MTV = \frac{((t_{sk} - t_{eq}/R_T) - a)}{b} \tag{4}$$

2.5. Experimental setup and procedure

The experiments were conducted in a large hall space at the HVAC laboratory at Aalto University. The hall layout and experimental setup are shown in Fig. 3. The different variants of the floor heater system were used at the task area under a lowered ambient temperature around 18 °C. The thermal manikin 'Therminator' was employed with the *MSP* control mode to verify the fulfillment of the thermal comfort criteria at each test.

The energy consumption by each system variant was periodically measured over the whole experiment period using a domestic electricity meter (analog meter). This was used to estimate the variant's power under steady-state operation. The surface temperature of the floor tiles was controlled using

Table 1
Mean vote ranges of the comfort zones and the correspondent sensations.[a]

Mean vote range	Thermal sensation
+1.5:+3.0	Too hot
+0.5:+1.5	Hot but comfortable
−0.5:+0.5	Comfort
−1.5:−0.5	Cold but comfortable
−3.0:−1.5	Too cold

[a] Given by Nilsson [12].

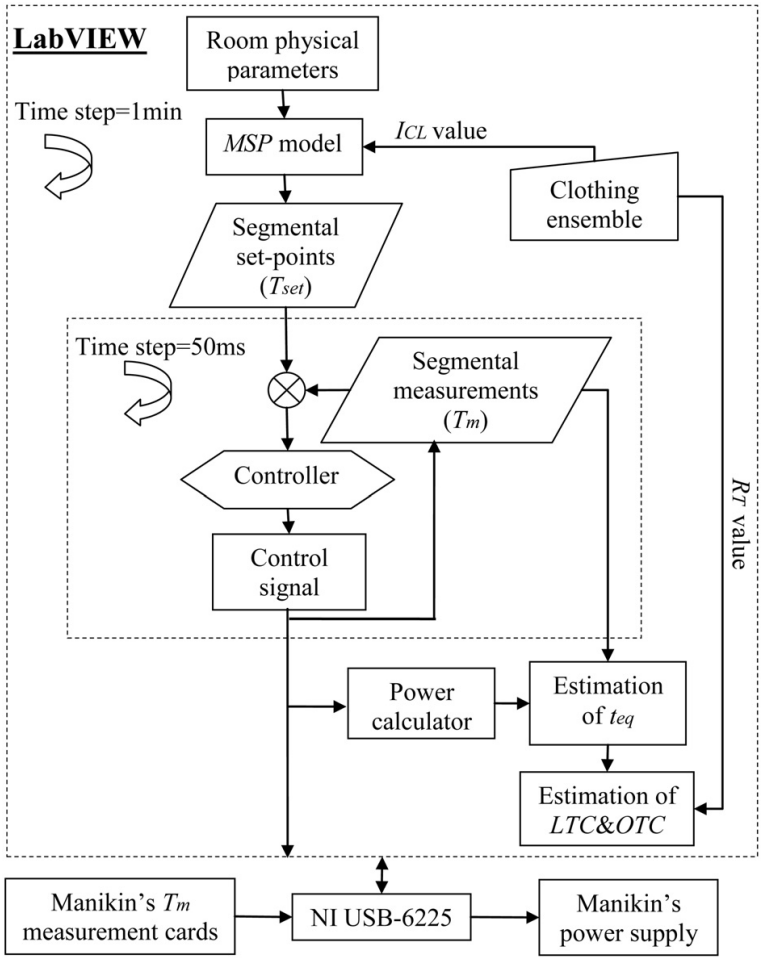

Fig. 2. Flow chart of the manikin's control system.

a proportional–integral–derivative (PID) temperature controller (TTM-04SP, Toho Elec. Inc.). An infra-red camera (ThermaCam-P60, Flir Systems Inc.) was used to calibrate the surface temperature of the floor tiles and obtain the average mean value for each system variant. A constant air volume/variable air temperature (CAVVAT) control scheme of the supply air was used with the general ventilation system to maintain the planned ambient condition at the hall space. However, fluctuations of air temperature and velocity as well as temperature gradients can expectedly occur in such a large hall space. In pilot tests, these room physical parameters were evaluated. Generally, the mean air velocity in the hall (at 0.6 m height) was around 0.15 m/s with turbulence intensity of 20%. The mean ambient temperature in the hall (at 0.6 m height) was around 18 °C (SD = 0.1) with a vertical temperature gradient of 1 K between 0.1 and 1.1 m height. Fig. 4 shows typical fluctuations at the hall space of air temperature and velocity measured over 5 h duration with a 10 s time step.

The use of the MSP control mode with the manikin measurements in a dynamic mode aimed at accounting for these fluctuations and interacting accurately with the surrounding environment. In addition, the experiments were carried out in the evenings to have nearly fixed internal gains and enhance the relevance of the comparisons between the different system variants.

In all procedures, the manikin wore a clothing ensemble that consists of: under-shirt, shorts, denim trousers, long-sleeve shirt, calf-length cotton socks and shoes. The clothing intrinsic thermal insulation value was measured (0.6 clo) according to ISO9920 [18] regulations using the manikin with the sitting posture under uniform conditions in a controlled environment. This measurement accounted for the insulation of a regular office armchair that has a short back-rest.

Online measurements of the indoor conditions were carried out during the whole experimental procedures. The air velocity was measured, at 3 different heights in the task area, using transducers (8465/75, TSI Inc.). The air and operative temperatures, at same heights, were measured using thermocouples and globe thermometers (T type, accuracy ±0.5 K). This was used to calculate the radiant temperature at the same three heights according to ISO7726 [19]. The measurements at the task area were connected through the manikin's data acquisition interface (NI USB-6225,

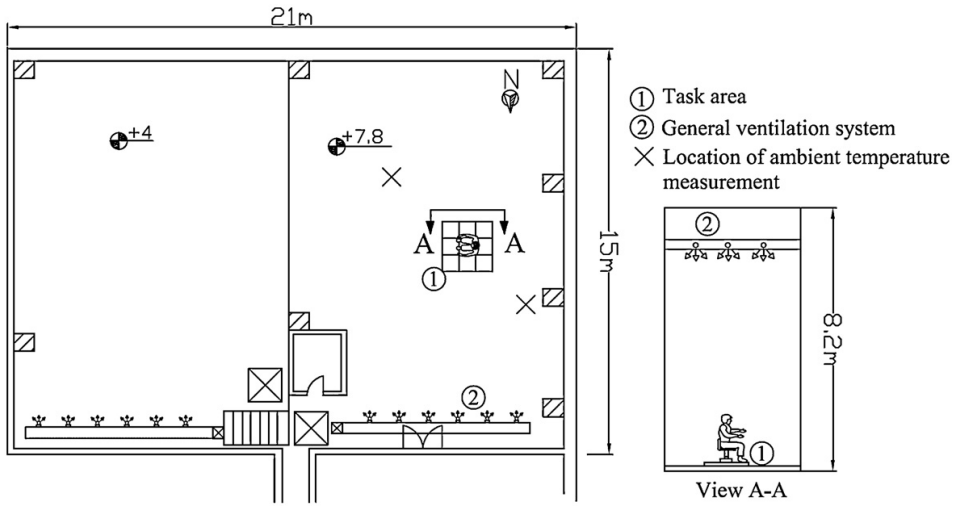

Fig. 3. Hall layout and experimental setup.

National instruments). These measurements averaged over 1 min interval were used with the manikin's MSP control. Furthermore, the ambient temperature was measured using thermistors (U type, Grant instruments) at same 3 heights from two locations in the hall (shown in Fig. 3). Airflow indicator kit (CH00216, Dräger Tube) was randomly used during the experiments at the task area to visualize the air movements. Generally, horizontal air draughts were observed at the task area below 0.6 m height and toward the north direction (see Fig. 3). The relative humidity (*RH*%) was around 30% during all experiments. This was measured using a humidity indicator (HM141, Vaisala). The ambient measurements were connected through a data acquisition unit (Squirrel SQ2040, Grant instruments) and were recorded at 10 s time interval. The average outdoor temperature during the time of the experiments in January 2012 was −2 °C (SD = 2 K).

A test procedure normally started by: setting the floor variant at a certain surface temperature, meanwhile the thermal manikin was operated in active mode and then the data was collected for approximately 1 h when the manikin/floor system reached steady-state and stabilized at the target temperature. The same procedure was then repeated with another surface temperature in case the selected surface temperature did not fulfill the comfort criteria. All measurements were connected on a personal computer and were monitored by the authors during the whole experimental procedures.

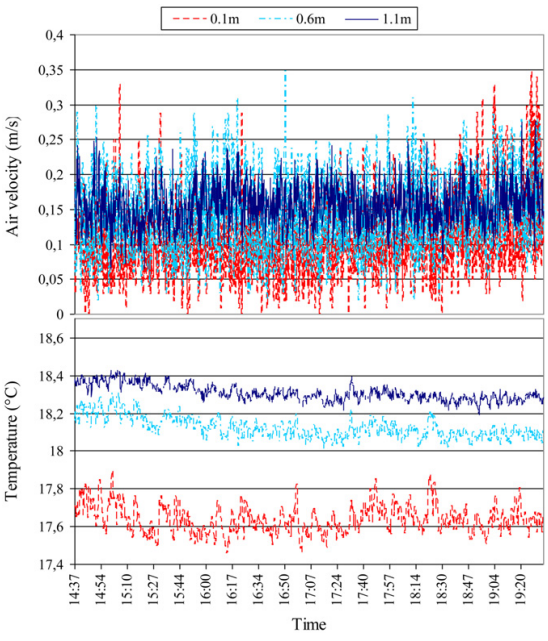

Fig. 4. Fluctuations in ambient temperature and air velocities at the hall space.

3. Results and discussion

3.1. Room physical parameters and manikin's operation

The experimental setup in the hall space aimed at testing the system variants under real-life conditions. Measurements of air temperature and velocities at the hall space in pilot tests showed considerable fluctuations of the measured quantities (see Fig. 4). This clearly represented a challenge for the relevance of the comparisons between the different system variants. Therefore, the room physical parameters were closely monitored before and during the experiments to judge the quality of the recorded data. Fig. 5 shows the measured data and standard deviation (SD) under the conditions by the different system variants. The ambient temperatures at the 3 different heights (Fig. 5a) were averaged from measurements at two locations in the hall space. The SD of the ambient temperature at 0.1 and 0.6 m heights was around 0.1 K while it was around 0.05 at 1.1 m height. The measurements of the ambient temperature indicate nearly similar ambient conditions at the different experiments and support the relevance of these comparisons. The measurements at the task area of air temperature, globe temperature and air velocity (Fig. 5b–d) are partly dependent on the conditions created by the system variants and were also affected by the variants' size and the positioning of the measurement instruments. The measured air temperature at 0.1 m height was in a range from 18.1 to 18.7 °C and showed relatively high

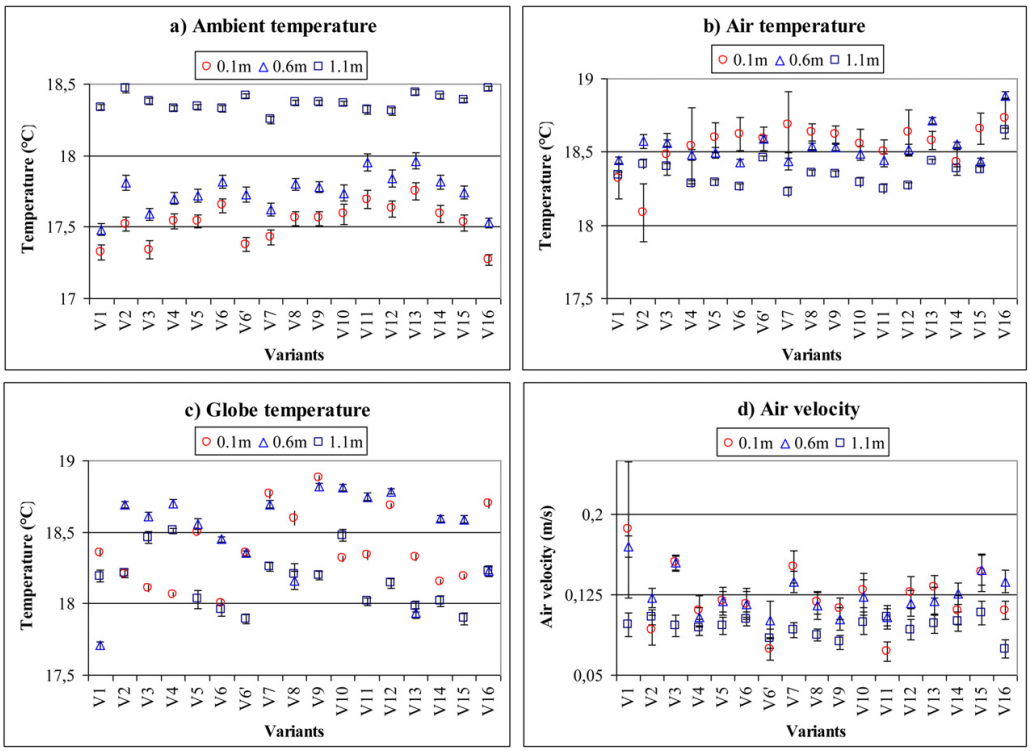

Fig. 5. Measured physical parameters of ambient and task area.

fluctuations (SD from 0.1 to 0.5 K). The measured temperatures at 0.6 m and 1.1 m were around 18.5 °C (SD ≈ 0.1 K). The measured globe temperatures at the 3 heights in the task area were in a range from 18 to 19 °C (SD ≈ 0.05 K). The air velocities were around 0.12 m/s at the 3 heights with SD 0.02 m/s. The highest air velocity recorded was at 0.1 m height under conditions by variant (V1) at which the fluctuations were also most high (SD = 0.13 m/s). Generally, an increase of nearly 1 K in the air temperature, compared to ambient, was realized in the task area at 0.1 and 0.6 m heights. The measured air temperatures at 1.1 m height at the task area were nearly similar to the ambient air temperatures at same height. This may indicate less influence of the floor-heating system at that height and under the described conditions in the hall space. However, this may still be confirmed out of the thermal manikin's measurements.

While the room physical parameters measured by the described instruments may be used to estimate directly the level of the thermal comfort, still a physical thermal manikin with the shape of human body is the most accurate tool to evaluate this quantity. The thermal manikin simulates adequately the human physical presence and with the human thermoregulatory control (i.e. *MSP* control) used, it can simulate well the human thermal presence in space. The measurements at the task area were connected with the manikin's system to dynamically interact with the surrounding environment at 1 min time step. That 1 min long time step was chosen to allow the control system enough time to respond. Based on the heat losses over that 1 min step, the equivalent temperature (t_{eq}) and correspondent LTC and OTC indices are instantaneously calculated using Eq. (4) (as the *MTV* value) and shown on the system's front panel in LabVIEW. Table 2 shows the coefficients used in Eq. (4); and the mean, min and max values of the segmental skin temperature under the different experiments. Fig. 6 shows an example of the dynamics of the manikin's segmental temperature under conditions by one of the system variants (i.e. V11). Fig. 6 from a to d shows the changes in skin temperature of head; trunk

Table 2
Parameters used in the comfort calculation and manikin's skin temperature distribution in the experiments.

Segment[a]	Parameters used in Eq. (3)			Skin temperature (°C)		
	RT (m² K/W)	a^b	b^b	Mean	Min	Max
Head	0.20	65.5	−33.9	33.61	33.46	33.80
UR back	0.25	36.1	−20.5	34.68	34.44	34.99
UL back	0.25	36.1	−20.5	34.68	34.44	34.99
R chest	0.28	36.1	−20.5	33.64	33.56	33.76
UR arm	0.24	43.0	−21.1	31.90	31.69	32.09
LR arm	0.24	43.0	−21.1	32.47	32.17	32.89
R hand	0.11	84.9	−57.2	26.19	25.81	26.89
L chest	0.28	36.1	−20.5	33.64	33.56	33.76
UL arm	0.24	43.0	−21.1	31.90	31.69	32.09
LL arm	0.24	43.0	−21.1	32.47	32.18	32.89
L hand	0.11	84.9	−57.2	26.19	25.81	26.89
R thigh	0.19	46.7	−20.3	29.25	28.98	29.74
R leg	0.18	46.7	−20.3	29.66	29.32	30.08
R foot	0.22	46.7	−20.3	29.82	29.40	30.38
L thigh	0.19	46.7	−20.3	29.25	28.98	29.74
L leg	0.18	46.7	−20.3	29.66	29.32	30.08
L foot	0.22	46.7	−20.3	29.82	29.40	30.38
LR back	0.25	36.1	−20.5	33.26	33.10	33.40
LL back	0.25	36.1	−20.5	33.26	33.10	33.40
Pelvis	0.34	39.5	−19.5	32.69	32.60	32.80
Overall	0.21	43.8	−13.3			

[a] L = left, LL = lower left, LR = lower right, R = right, UL = upper left and UR = upper right.
[b] Values are obtained from Nilsson [12].

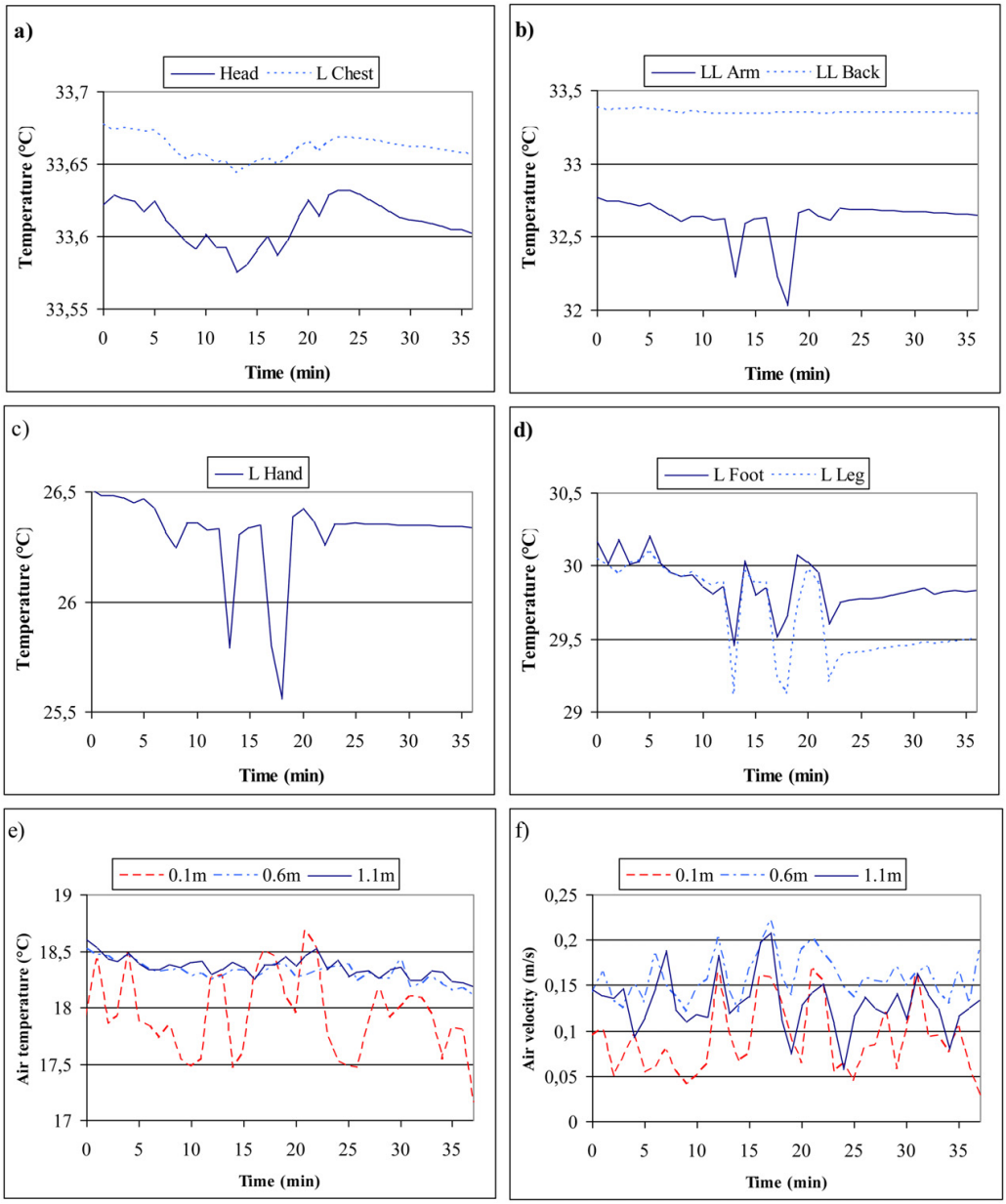

Fig. 6. Dynamics of the manikin's segmental skin temperature and correspondent room physical parameters under experiment of variant V11.

segments as: chest and lower back; and body limbs segments as: lower arm, hand, leg and foot. Fig. 6e and f shows the measured air temperature and velocity respectively, over the same duration. In this example, the globe temperature was nearly constant with SD around 0.05 K. As can be seen, the fluctuations in the physical parameters affected more the limbs' segments. While slight changes in the skin temperature of head and chest segments were recorded for the interaction with the surrounding environment, the lower back segments remained nearly constant as they were well insulated by the seat back-rest.

3.2. Thermal comfort

The local and overall comfort under the conditions created by the floor-heating system variants were estimated using the t_{eq} approach and Nilsson's model (Eqs. (3) and (4)). Fig. 7 shows the segmental and overall mean thermal votes (*MTV*) measured by the thermal manikin for all system variants. The figure was subdivided into 6 subfigures to help improve the visibility of the data. Fig. 7a shows the results of the largest and smallest variants while the subfigures from b to f gather variants with the same surface area.

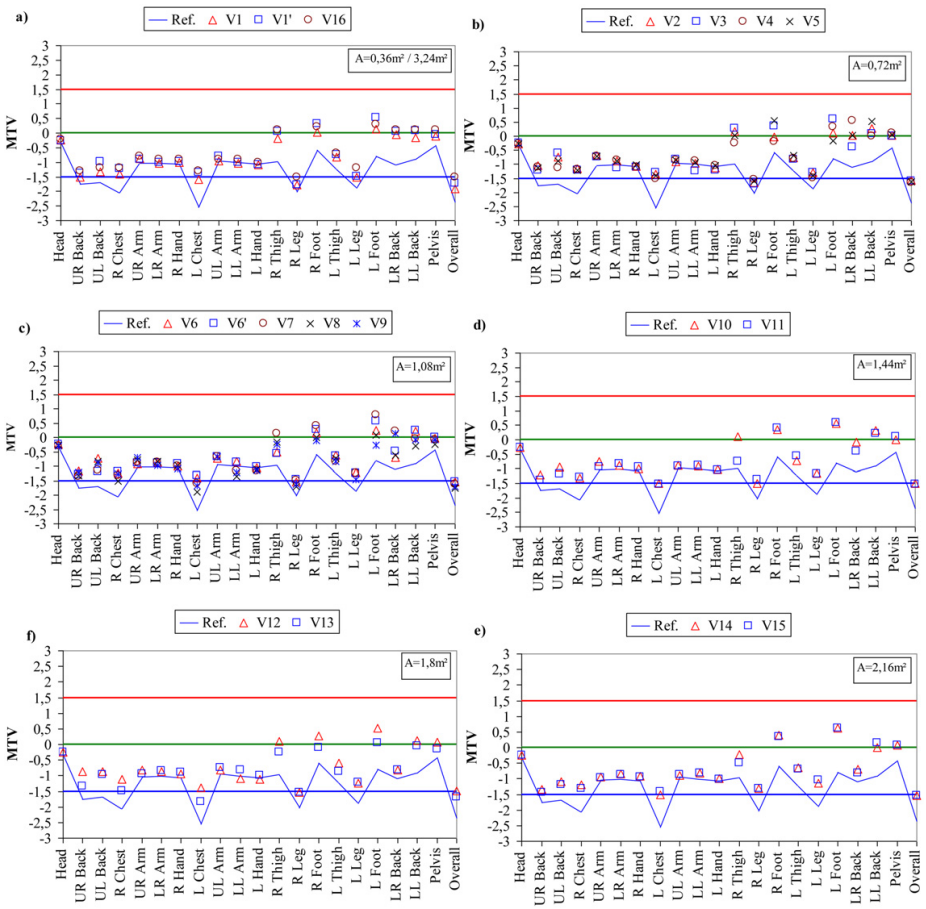

Fig. 7. Segmental and overall mean thermal votes (*MTV*) measured by the thermal manikin for all tested variants.

Table 3
Segmental and overall *MTV* values measured by the thermal manikin for the different variants.

Segment[a]	Ref.	V1	V1′	V2	V3	V4	V5	V6	V6′	V7	V8	V9	V10	V11	V12	V13	V14	V15	V16
Head	−0.3	−0.3	−0.3	−0.3	−0.2	−0.3	−0.3	−0.2	−0.2	−0.3	−0.3	−0.3	−0.3	−0.27	−0.2	−0.3	−0.3	−0.2	−0.2
UR back	−1.8	−1.5	−1.4	−1.0	−1.2	−1.1	−1.1	−1.2	−1.3	−1.4	−1.3	−1.2	−1.2	−1.41	−0.9	−1.3	−1.3	−1.4	−1.3
ULback	−1.7	−1.3	−1.0	−0.7	−0.6	−1.1	−0.9	−0.7	−1.2	−1.1	−0.8	−0.9	−0.9	−1.19	−0.9	−1.0	−1.1	−1.2	−1.2
Chest R	−2.0	−1.4	−1.2	−1.2	−1.2	−1.2	−1.2	−1.2	−1.2	−1.3	−1.5	−1.3	−1.3	−1.28	−1.1	−1.5	−1.2	−1.3	−1.2
UR arm	−1.0	−0.9	−0.9	−0.7	−0.8	−0.7	−0.7	−0.9	−0.9	−0.9	−0.8	−0.7	−0.7	−0.95	−0.8	−0.9	−0.9	−1.0	−0.8
LR arm	−1.0	−1.0	−1.0	−0.9	−1.1	−0.9	−0.9	−0.9	−0.9	−0.9	−0.8	−1.0	−0.9	−0.84	−0.9	−0.8	−0.8	−0.9	−0.9
Hand R	−1.1	−1.0	−1.0	−1.1	−1.1	−1.1	−1.0	−1.0	−0.9	−1.0	−1.0	−1.1	−1.0	−0.94	−0.9	−0.9	−0.9	−0.9	−0.9
Chest L	−2.5	−1.6	−1.4	−1.4	−1.3	−1.5	−1.4	−1.4	−1.3	−1.6	−1.9	−1.7	−1.5	−1.54	−1.4	−1.8	−1.5	−1.4	−1.3
UL arm	−1.0	−1.0	−0.8	−0.9	−0.8	−0.8	−0.9	−0.7	−0.7	−0.7	−0.7	−0.7	−0.9	−0.92	−0.8	−0.7	−0.9	−0.9	−0.9
LL arm	−1.0	−1.0	−1.0	−1.0	−1.2	−0.9	−0.9	−0.8	−0.9	−1.2	−1.4	−1.2	−0.9	−0.89	−1.1	−0.8	−0.8	−0.8	−0.9
Hand L	−1.1	−1.1	−1.1	−1.1	−1.2	−1.0	−1.1	−1.1	−1.0	−1.2	−1.1	−1.1	−1.0	−1.05	−1.1	−1.0	−1.0	−1.0	−1
Thigh R	−1.0	−0.2	0.1	0.2	0.3	−0.3	0.0	−0.5	−0.6	0.1	−0.2	−0.3	0.1	−0.76	0.1	−0.2	−0.2	−0.5	0.1
Leg R	−2.0	−1.8	−1.8	−1.7	−1.7	−1.5	−1.6	−1.5	−1.5	−1.5	−1.7	−1.6	−1.5	−1.36	−1.5	−1.5	−1.3	−1.3	−1.5
Foot R	−0.6	0.0	0.3	0.0	0.4	−0.2	0.6	0.2	0.3	0.4	0.0	−0.1	0.4	0.39	0.3	−0.1	0.4	0.3	0.2
Thigh L	−1.2	−0.8	−0.7	−0.8	−0.8	−0.8	−0.7	−0.6	−0.7	−0.8	−0.7	−0.8	−0.7	−0.56	−0.6	−0.9	−0.6	−0.7	−0.7
Leg L	−1.9	−1.5	−1.5	−1.3	−1.3	−1.5	−1.4	−1.2	−1.2	−1.2	−1.5	−1.5	−1.2	−1.18	−1.2	−1.2	−1.1	−1.1	−1.2
Foot L	−0.8	0.1	0.5	0.1	0.6	0.3	−0.2	0.2	0.6	0.8	0.1	−0.3	0.6	0.60	0.5	0.1	0.6	0.6	0.3
LR back	−1.1	0.0	0.1	0.0	−0.4	0.5	0.0	−1.0	−0.5	0.2	−0.6	0.1	−0.1	−0.41	−0.8	−1.0	−1.1	−0.8	0.1
LL back	−0.9	−0.2	0.1	0.3	0.1	0.0	0.5	0.2	0.3	−0.1	−0.3	−0.1	0.3	0.21	0.1	0.0	0.0	0.2	0.1
Pelvis	−0.4	−0.1	−0.1	0.0	0.0	0.1	0.1	0.0	0.0	−0.1	−0.2	−0.1	0.0	0.11	0.1	−0.1	0.1	0.1	0.1
Overall	−2.4	−1.9	−1.7	−1.6	−1.6	−1.7	−1.6	−1.5	−1.5	−1.6	−1.8	−1.7	−1.5	−1.54	−1.5	−1.7	−1.5	−1.5	−1.5

[a] L = left, LL = lower left, LR = lower right, R = right, UL = upper left and UR = upper right.

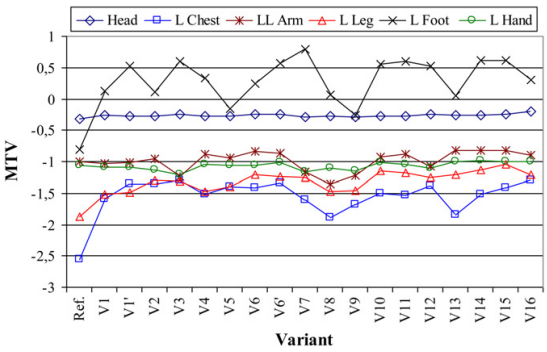

Fig. 8. Thermal comfort level of different body segments under the conditions by the tested variants.

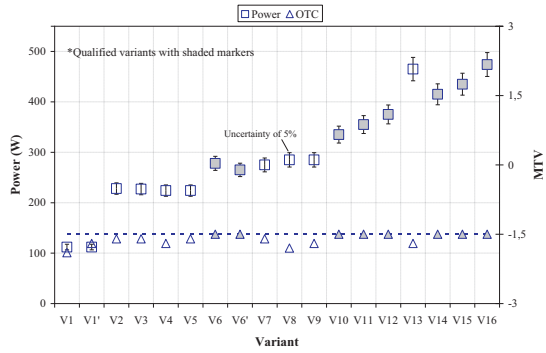

Fig. 9. Measured power and attained OTC level of the experimented variants.

The *MTV*'s for a reference condition with no local heating and the borders of the comfort criteria (adopted from Nilsson's model) are marked on all subfigures. The results are also tabulated in Table 3 to numerically clarify the given data on the figure. As can be seen, less than half of the experimented variants could fulfill the comfort criteria. The comfort level was near to the lower bound of the comfort criteria (i.e. −1.5) at the upper back, chest and leg segments while it was mostly around neutral at other segments such as lower back, thigh, foot and pelvis.

In order to further analyze the comfort results away from the comfort criteria, Fig. 8 shows the comfort levels under the conditions by the different variants for some of the body segments. These represent body segments of the head, trunk, upper and lower limbs to indicate the changes in comfort level at different heights in the task area. As can be seen, at the head level the change in the comfort level was minor. The maximum difference in the t_{eq} from the reference case (with no local heating) was 0.8 K particularly under the conditions by the largest variant (V16). This may suggest that the thermal plumes at the task area were affected by the observed air draughts (see Section 2.5) and the heat transfer at that height was mainly due to the heated surface area and radiation. Then, it can be stated that the head segment was more affected by the ambient condition in these experiments; however, the comfort level of the head (according to the t_{eq} approach) was near to neutral under this ambient condition. The upper limbs, stretched to the front, were also affected more by the ambient condition but remained in the acceptable range of the comfort criteria. As shown in Fig. 8, the change in the comfort level of the lower arm and hand compared to the reference case was minor and even in some cases it was slightly negative. Conversely, the local floor-heating succeeded to improve the comfort level of the chest and leg segments by 0.5–1° on the comfort scale. The comfort level of the foot segment illustrates well the differences of the floor temperature and geometries of the system variants. The highest *MTV* values (from 0.5 to 0.8) were obtained when the feet were surrounded by heated tiles with surface temperature of 40 °C, while the lowest were at the reference condition and when placed on non heated tiles (e.g. V5 and V9). The foot comfort level with the shoes was in a range from −0.8 to 0.8 and apparently it was not much affected by the high surface temperature of the floor or by the lowered ambient conditions.

3.3. Optimum configuration

The experiments were carried out to evaluate the performance and find the optimum configuration including geometry, surface area and temperature from the different floor-heater variants under the described conditions in the hall space. The local and overall comfort levels measured by the thermal manikin were the driver of the performance evaluation of these system variants. The optimum surface temperature for each variant was experimentally found subject to the thermal comfort criteria and limited by the allowed maximum floor temperature. The difficulty of finding that optimum temperature was lessened by experimenting at first the largest and the smallest variants to define a searchable range. Then, it was easier to find the temperature for the rest of the variants guided by their surface area and using a degree or half a degree step in that range. The allowed maximum floor temperature (i.e. 40 °C) was not sufficient to fulfill the comfort criteria for all variants with 1 or 2 tiles. Furthermore, it was neither sufficient for most of the 3 tiles variants nor for the "X" shape variant (V13). Generally, the optimum surface temperatures of the qualified variants were in a range from 31 to 40 °C. Table 4 gives the characteristics of the different system variants including the surface temperatures, power and the order of optimum configurations. Fig. 9 shows the measured power of each system variant and the overall thermal comfort (OTC) realized under these system variants. The figure shows the qualified variants with shaded markers and a dotted line for the lower bound of the OTC. Error bars were used on the figure with the measured powers to indicate uncertainty of 5% in this measurement with the analog electricity meter used.

Generally, the surface area of the heated floor was proportionally correlated with the surface temperature. This was physically consistent with respect to radiant and convective heat transfer phenomena. The geometry of the variants had a clear impact on the results. For example, variants with the same surface area (e.g. V14, V15 and V10, V11) required different surface temperatures to fulfill the comfort criteria. Furthermore, variants with the same surface area (e.g. V6, V7 and V12, V13) fulfilled or did not fulfill the comfort criteria. Additionally, variants with considerable difference in the surface area as V14 and V16 required surface temperatures of only 1 K difference (i.e. 32 and 31 °C, respectively) to fulfill the comfort criteria. Based on these experimental results, it was found that careful geometrical planning of a heated floor area around a seated person can lead to energy-efficiency and be more effective pertaining to thermal comfort. The heated floor posterior to the manikin position was less beneficial since the body from that side was mostly insulated by the seat back-rest. This was clearly manifested from results of different variants (e.g. V14 and V15). In addition, the heated floor diagonally placed against the manikin's position was also proven to be less beneficial when compared the results from V1 with V8 or V9 results. On the other hand, the heated floor on the sides and anterior to the manikin position was proven to be most effective. The experiments of variants V1 and V1′ showed that the placement of a heated tile under the seated manikin was less effective than with the anterior position. With variant V1′, the

Table 4
Characteristics of the experimented floor-heating system variants and optimum configurations.

Variant	Surface area, A (m^2)	No. of tiles	Floor temperature, Ts (°C)	Comfort criteria	Power (W)	Order of optimum configurations
1 and 1′	0.36	1	40		112	
2	0.72	2	40		228	
3	0.72	2	40		227	
4	0.72	2	40		224	
5	0.72	2	40		224	
6	1.08	3	40	×	277	2
6′	1.08	3	39	×	265	1
7	1.08	3	40		278	
8	1.08	3	40		285	
9	1.08	3	40		285	
10	1.44	4	37	×	335	3
11	1.44	4	38	×	355	4
12	1.80	5	36	×	375	5
13	1.80	5	40		465	
14	2.16	6	32	×	415	6
15	2.16	6	34	×	435	7
16	3.24	9	31	×	474	8

OTC was improved by 0.2 on the comfort scale compared to variant V1. Then based on this finding and when variant V6 was found to fulfill the comfort criteria, we formulated the variant V6′ and expected further better energy performance. The variant V6′, as expected, fulfilled the comfort criteria with the least system power.

Based on the verifications carried out, these findings may be generalized to similar types of spaces. However, they are partly related to the experimental setup described and may have been partly influenced by the direction of the air movements at the task area. In these experiments, the lower bound (i.e. −1.5) of the acceptable comfort range [12] was used in the comfort criteria with that light summer clothing (0.6 clo) of the manikin. Then with winter clothing used normally indoors, these system variants with the suggested surface temperatures may provide higher comfort level or can be optimized to operate with lower surface temperatures. These results were mainly for a single seated person and may need further investigations before application for multiple persons. However, this localized system with individual control enabled according to certain limits, may easily be utilized for a single or multiple application. It should be noted that the measured power of these variants may further be reduced by optimizing the construction and the heating method of the floor. The scope of this study was mainly to find the optimum configuration related to geometry, surface area and temperature. Conversely, the energy-saving due to the use of this localized system (based on current construction) along with the set-point reduction of room temperature (i.e. 3 K) was estimated for the shopping mall's application. This was carried out based on our hall's characteristics and using the dynamic building energy simulator IDA ICE 4.1. In the simulation, 10% of the hall area was assumed to be the mall's resting spots with localized heating. The simulation indicated that the monthly saving compared to conventional system was in a range from 10 to 65% while the total annual saving was 17%. The lowest savings were at extreme winter conditions while the highest were at summer, spring and autumn heating demand.

The illustrated methodology may also be implemented in the design of other types of localized HVAC systems towards energy-efficiency and thermal comfort in buildings.

4. Conclusions

The objective of this work was to obtain the optimum geometry, surface area and temperature of a localized floor heater that minimize the energy use and fulfill thermal comfort criteria. An experimental technique using a thermal manikin was developed to test 18 different variants of localized floor heater. The experiments showed that the geometry of the heated floor had a clear impact on the effectiveness pertaining to thermal comfort; and hence, the energy-efficiency. Generally, enlarging the surface area of a heated floor contributes in reducing the required surface temperature for the fulfillment of comfort. However, this can further be optimized by investigating the proper geometry of that heated floor. The heated floor posterior, under the seat and diagonally placed subject to the manikin position was proven to be less effective compared to heated floor on the sides and anterior to the manikin position. The optimum configuration that fulfilled the comfort criteria with the least measured steady-state power consisted of 3 heated tiles surrounded the manikin from the two sides and anterior position. The total surface area of that variant was nearly 1 m^2 while the required surface temperature was around 39 °C. The power of this localized system may further be reduced by optimizing the construction and the heating method of the floor. This system with individual control enabled according to certain limits, may easily be utilized for a single seated person and for multiple application. The annual energy-saving due to the use of this localized system (based on current construction) in shopping malls was estimated to be around 17% compared to conventional systems.

The experimental setup in a large hall space mainly intended to simulate a task area in the shopping mall's application; however, these results may also be useful for industrial buildings. It should be noted that these results may be partly related to our experimental setup including the ambient condition and the used clothing ensemble. Moreover, it may also have been partly influenced by the direction of air movements in the hall space. The used methodology may be implemented similarly in the design of other types of localized HVAC systems towards energy-efficiency and thermal comfort in buildings.

Future work will include further testing of localized HVAC systems under different indoor conditions.

Acknowledgment

The authors acknowledge the financial support kindly provided by Aalto University MIDE project.

References

[1] N.Z. Azer, R.G. Nevins, Physiological effects of locally cooling the head in a 95F and 75%RH environment, ASHRAE Transactions 2297 (1974) 93–100.
[2] F. Bauman, et al., Testing and optimizing the performance of a floor-based task conditioning system, Energy and Buildings 22 (1995) 173–186.
[3] H. Amai, et al., Thermal sensation and comfort with different task conditioning systems, Building and Environment 42 (2007) 3955–3964.

[4] E. Arens, et al., Partial- and whole-body thermal sensation and comfort – Part I: uniform environmental conditions, Thermal Biology 31 (2006) 53–59.
[5] E. Arens, et al., Partial- and whole-body thermal sensation and comfort – Part II: non-uniform environmental conditions, Thermal Biology 31 (2006) 60–66.
[6] H. Zhang, et al., Comfort, perceived air quality, and work performance in a low-power task-ambient conditioning system, Building and Environment 45 (1) (2010) 29–39.
[7] S. Watanabe, et al., Thermal evaluation of a chair with fans as an individually controlled system, Building and Environment 44 (2009) 1392–1398.
[8] R. Sørlie, et al., Maintaining acceptable thermal comfort with a low air temperature, by means of local heating, in: Indoor Air Congress, Helsinki – Finland, 1993.
[9] S. Stensson, M. Axell, K.P. Småge, P. Fahlén, Specific energy use in Swedish and Norwegian shopping malls, in: Proceedings of ECEEE 2009 Summer Study, Nice, France, 2009.
[10] ISO Ergonomics of the Thermal Environment, Analytical Determination and Interpretation of Thermal Comfort Using Calculation of the PMV and PPD Indices and Local Thermal Comfort Criteria, Standard ISO 7730:2005, International Organization of Standardization, Geneva, Switzerland, 2005.
[11] H. Nilsson, Comfort Climate Evaluation with Thermal Manikin Methods and Computer Simulation Models, PhD Thesis, 2004, ISBN: 91-7045-703-4.
[12] H. Nilsson, Thermal comfort evaluation with virtual manikin methods, Building and Environment 42 (2007) 4000–4005.
[13] E. Foda, K. Sirén, A new approach using Pierce two-node model for different body parts, International Journal of Biometeorology 55 (4) (2011) 519–532.
[14] E. Foda, K. Sirén, A thermal manikin with human thermoregulatory control: implementation and validation, International Journal of Biometeorology (2011), http://dx.doi.org/10.1007/s00484-011-0506-6.
[15] D.P. Wyon, S. Larsson, B. Forsgren, I. Lundgren, Standard Procedures for Assessing Vehicle Climate with a Thermal Manikin, SAE, Paper 89004, 1989.
[16] D.P. Wyon, M. Sandberg, Thermal manikin prediction of discomfort due to displacement ventilation, ASHRAE Transactions 96 (1) (1990) 67–75.
[17] T. Bedford, The Warmth Factor in Comfort at Work, MRC Industrial Health Board Report 76, HMSO, London, UK, 1936.
[18] ISO Ergonomics of the Thermal Environment, Estimation of the Thermal Insulation and Water Vapor Resistance of a Clothing Ensemble, Standard ISO 9920:2007(E), International Organization of Standardization, Geneva, Switzerland, 2007.
[19] ISO Thermal Environment, Instruments and Methods for Measuring Physical Quantities, Standard ISO 7726:1985(E), International Organization of Standardization, Geneva, Switzerland, 1985.